

Correlations Between Creep, Shrinkage, and Dynamic Mechanical Characteristics of Magnetic Tape Materials

Brian L. Weick

Department of Mechanical Engineering, School of Engineering and Computer Science,
University of the Pacific, Stockton, California 95211

Received 26 January 2010; accepted 27 June 2010

DOI 10.1002/app.33032

Published online 13 October 2010 in Wiley Online Library (wileyonlinelibrary.com).

ABSTRACT: Creep compliance, shrinkage, and dynamic mechanical analysis (DMA) results are presented and discussed for developmental magnetic tapes made from PEN and metalized PET (Spaltan[®]) substrates as well as PEN substrate samples cut from wide-stock in the machine and transverse directions. Curve fit parameters from the Kelvin-Voigt model are discussed to shed light on the creep-compliance characteristics, particularly the roll-off characteristics observed at elevated temperatures and long time periods. Characteristic peaks observed in storage and loss

moduli measured using DMA that correspond with molecular movement provide information that assists with the understanding of creep-compliance and shrinkage behavior for these materials. Such movement corresponds with dimensional instabilities that need to be understood for future generations of advanced digital magnetic tapes. © 2010 Wiley Periodicals, Inc. *J Appl Polym Sci* 120: 226–241, 2011

Key words: creep; polyesters; viscoelastic properties; structure-property relations; PET; PEN

INTRODUCTION

Background

Archival storage of information continues to rely on advanced digital magnetic tapes. As summarized in the introduction to a recent article by Weick,¹ the dimensional stability of these tapes is crucial to meet long-term storage requirements. A 30+ year storage life is required to preserve crucial government and industrial data, and even 100+ year storage lives could be necessary for medical image applications such as magnetic resonance imaging, which not only requires the information to be stored for the lifespan of the patient but also involves relatively large file sizes that can take advantage of the storage volume of magnetic tapes and library systems.

Typical storage environments for tapes manufactured to the linear tape open (LTO) format are 16–32°C with a 20–80% relative humidity,² and therefore, it is important to understand the properties and characteristics of materials that comprise magnetic tapes including the front coat consisting of a magnetic and nonmagnetic layer, a substrate, and back coat. This is particularly important when the high-track density across the tape measured in tracks-per-inch (TPI) is considered for advanced tapes. The TPI for tapes such as LTO has more than

doubled in the last 10 years from 923 TPI in 2000 for LTO1 to 2228 TPI in 2007 for LTO4 and LTO5 tapes have more than 3000 TPI. Other commercial formats have seen similar increases in TPI.¹

Because magnetic tapes undergo widthwise contraction (or expansion) when they are stored in reels due to the viscoelastic characteristics of the materials that comprise the tape, it is important to perform experimental studies that enable a fundamental understanding of the viscoelastic characteristics of these materials. These studies include creep-compliance measurements with a custom-built test apparatus, and dynamic mechanical analysis (DMA) using commercially available test equipment. The measurements not only yield quantifiable parameters such as creep compliance along with the storage and loss moduli with $\tan(\delta)$ as the ratio of the two moduli, but they also provide a phenomenological understanding of the polymer characteristics that enable (or perhaps disable) the effective storage of information on magnetic tapes.

Objectives

An understanding of the differences between the viscoelastic characteristics of metalized PET (Spaltan[®]) and PEN substrates as well as tapes made from these substrates is an important goal of this study. Characteristic shapes of the creep-compliance curves at elevated temperature levels along with curve fit parameters from the Kelvin-Voigt (K-V) model can enable this understanding, and more specifically, correlations

Correspondence to: B. L. Weick (bweick@pacific.edu).

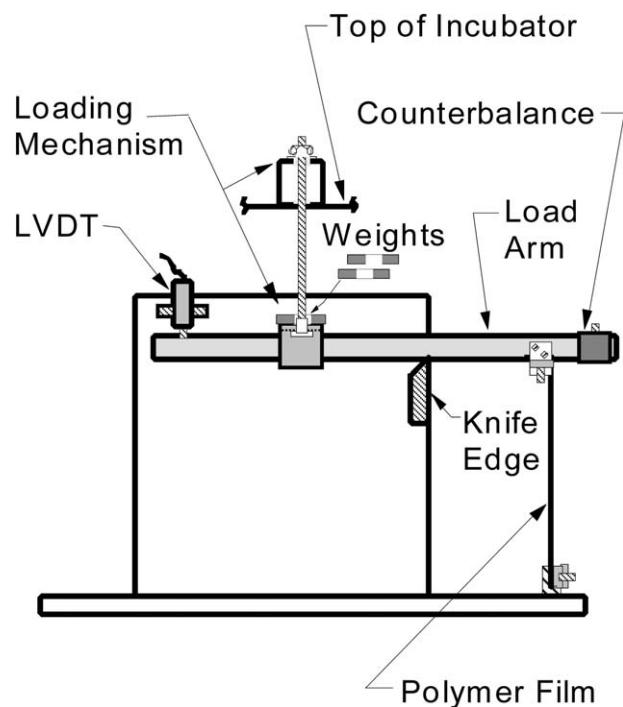


Figure 1 Schematic view of a creep tester for evaluating the creep behavior of magnetic tape materials.

between the creep-compliance data and representative characteristics of the polymer-based tapes and substrates are desired. To learn about representative polymer characteristics that influence dimensional stability, a mature experimental technique called DMA can be performed. Primary and secondary relaxations that are temperature and frequency dependent can be measured, and DMA experiments performed with the metalized PET (Spaltan[®]) and PEN-based media can enable correlations with long-term creep-compliance data measured at elevated temperatures. Overall, media manufacturers and suppliers can use this information to develop improved substrate and tape products with documented dimensional stability characteristics, and drive manufacturers can use the

information to develop improved methods for writing and reading information from tape media.

Experimental and analytical procedure used for creep experiments

Creep experiments were performed with a custom-built apparatus housed in a temperature-controlled incubator. A schematic of this test apparatus is shown in Figure 1. Humidity was controlled by using desiccant in the test chamber at low temperatures (30°C); at high temperatures (50 and 70°C) the chamber dries out and the humidity was <1%. Test samples that were typically 330 to 400 mm long were evaluated. The samples had 200 mm long test sections and were 12.7-mm wide. Environmental conditions were monitored using a hygrometer and temperature sensor, and the test apparatus used linear variable differential transformers (LVDT's) connected to a LabView-based 16-bit A/D system to measure extension or contraction of the samples. The experiments were performed at a 7.0 MPa stress level that corresponds with typical drive tensions.

An outline of the experimental procedure and analytical techniques used to acquire and process data from the custom creep apparatus is described in Table I. Other articles by Weick^{1,3} and Weick and Bhushan⁴⁻⁶ provide a thorough description of these techniques, and will only be described briefly and expanded-on as necessary in this article.

Table II provides specifications for the magnetic tapes used in this study. Two developmental tape samples provided by Sony use a metalized polyester substrate manufactured by Toray that is comprised of poly (ethylene terephthalate) PET and a proprietary nanoengineered polymer blend. The trade name for this metalized PET substrate is Spaltan[®]. Tape Sample A uses a metalized PET (Spaltan[®]) substrate with a "thin" 0.05- μm thick metalized layer, and Tape Sample B uses a metalized PET (Spaltan[®]) substrate with a "thick" 0.1 μm thick layer. For simplicity, these

TABLE I
Outline of Experimental and Analytical Procedure

Perform creep-compliance experiments at 30, 50, and 70°C for 50 to 100+ h. At least three repeats are performed at each temperature level.
Use four different types of samples: (1) tape, (2) front coat + substrate, (3) substrate + back coat, and (4) substrate only. Layers are removed using methyl ethyl ketone (MEK).
Calculate time-dependent creep-compliance $D(t)$ and initial creep-compliance D_0 from repeat experiments at each temperature level.
Curve fit data to the K-V viscoelastic model using a Levenburg-Marquardt algorithm to determine and analyze viscoelastic properties.
Use time-temperature superposition to predict creep compliance for extended time periods (>100 years) at a reference temperature of 30°C.
Use a rule-of-mixtures approach to predict creep compliance for the front and back coats.
Predict rate of creep compliance using curve fit parameters. This rate of creep compliance can be referred to as creep velocity.
Compare results with known properties and characteristics of the constitutive tape materials to gain a more fundamental understanding of the dimensional stability of the materials.

TABLE II
Magnetic Tape and Substrate Sample Specifications

Sample designation and type of substrate	Supplier	Metalized layer thickness (each side), μm	Measured tape thickness, μm	Measured substrate thickness, μm	Elastic modulus (MD), GPa
Tape Sample A with metalized PET (Spaltan [®]) substrate	Sony	Thin, 0.05	6.67	5.10	7.7
Tape Sample B with metalized PET (Spaltan [®]) substrate	Sony	Thick, 0.1	6.65	5.09	8.4
PEN tape sample	Sony	–	6.60	4.99	7.8
Machine direction (MD) PEN substrate sample cut from wide-stock	Teijin-Dupont	–	–	5.00	–
Transverse direction (TD) PEN substrate sample cut from wide-stock	Teijin-Dupont	–	–	5.00	–

samples will be referred to as metalized PET A and metalized PET B, but it is understood that the substrates are actually Spaltan[®]. Sony also provided a development tape sample that uses a PEN substrate, and this tape is similar to LTO4. Wide-stock PEN substrate sheets supplied by Teijin-Dupont were also provided for the study. These wide-stock sheets enabled the fabrication of test samples in the machine (MD) and transverse (TD) directions.

Viscoelastic analysis method used for creep experiments

As outlined in Table I, creep-compliance experiments were performed at elevated temperatures using samples of magnetic tape materials. Using output from the LVDT's, the creep strain, $\varepsilon(t)$, can be determined as well as the creep compliance, $D(t)$, as the initial steps in the viscoelastic analysis.

$$\varepsilon(t) = \frac{\Delta l(t)}{l_0} \quad (1)$$

$$D(t) = \frac{\varepsilon(t)}{\sigma_0} = \frac{\Delta l(t)}{\sigma_0 l_0} \quad (2)$$

$\Delta l(t)$ is the change in length of the test specimen as a function of time, l_0 is the original length of the test specimen, $\varepsilon(t)$ is the amount of strain the film is subjected to, σ_0 is the constant applied stress, and $D(t)$ is the tensile creep-compliance of the test specimen as a function of time.

Examples of raw creep-compliance data for metalized PET tape and substrate samples are shown in Figure 2 along with results for the PEN substrates cut from wide-stock film in the MD and TD directions. Three repeat experiments are shown for each sample, and an average initial creep compliance, D_{0v} , is used to adjust for variation in initial loading.^{1,3} Overall, the metalized PET tape and substrate samples have a lower creep compliance when compared with the PEN substrate samples, and they also appear to have a lower creep rate as indicated by

their slopes. Furthermore, the metalized PET samples have a lower creep compliance compared with past results for unmetalized PET samples. However, the metalized PET creep-compliance curves tend to roll-off more at longer time periods. The PEN substrate samples follow classic viscolastic behavior. Note that the initial creep-compliance is lower for the PEN-TD sample, although the rate of creep compliance is similar for PEN-TD and PEN-MD as indicated by the slopes of the curves. At longer time periods, the PEN-TD sample seems to roll-off slightly more than the MD sample. The metalized PET tape seems to have a slightly higher overall creep compliance compared with the metalized PET substrate. This difference could be due to the compliant binder used in the front coat of the magnetic tape.

Creep-compliance data for the test specimens are modeled using a generalized K-V viscoelastic model, which has the following mathematical form:

$$D(t) = D_0 + \sum_{k=1}^K D_k [1 - \exp(-t/\tau_k)] \quad (3)$$

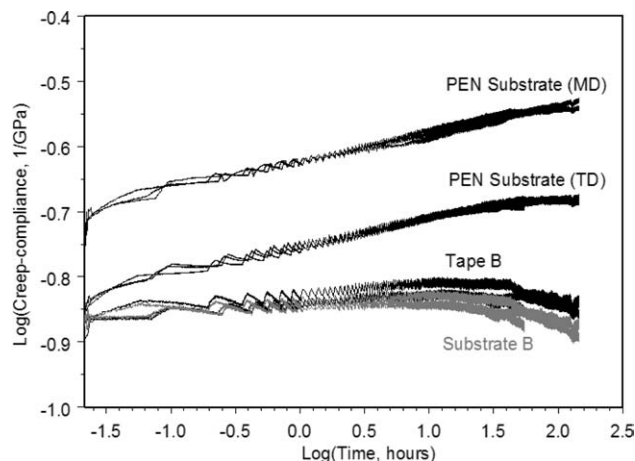


Figure 2 Raw creep-compliance data at 50°C for PEN substrate samples cut from wide-stock in the MD and TD compared with Tape and Substrate B samples that use metalized PET (Spaltan[®]) substrate material. Average D_{0v} values were used to adjust for variation in initial loading.

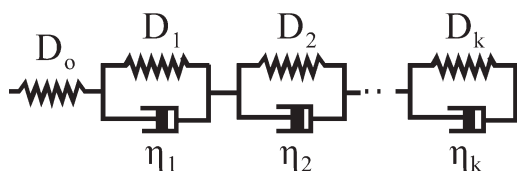


Figure 3 The K-V model used to express the elastic and viscous characteristics of polymeric materials.

where, D_0 is the instantaneous compliance at time $t = 0$, D_k is the discrete compliance term, and τ_k is the discrete retardation time for each K-V element.

Equation 3 is typically represented as a series of parallel springs and dashpots connected to a single spring. This mechanical analog is shown in Figure 3 and is indicative of a viscoelastic polymer, which has an amorphous phase with mainly unoriented molecules, and a crystalline phase, which contains oriented molecules. Components of the polymeric structure, which respond instantly to an applied stress are modeled as a single spring with an instantaneous compliance D_0 , which is inversely proportional to the elastic modulus, but should not be used as an exact substitute. Components of the polymeric structure which do not respond instantly but are deformed in a time-dependent manner are modeled as multiple elements consisting of springs and dashpots acting in parallel. Each element contains a spring which has a compliance D_k , and a dashpot with a viscosity equal to η_k . Compliances correspond with recoverable characteristics, and viscosities correspond with nonrecoverable characteristics. The retardation time for each k^{th} element is defined below:

$$\tau_k = \eta_k D_k \quad (4)$$

Note that the retardation time is directly proportional to the viscosity and compliance. As the retardation time increases, the exponential term goes to 1, and a rudimentary assessment of this means the influence of the entire K-V element should disappear. However, really large positive or negative retardation times do have a marked influence on the creep compliance. A relatively small compliance and large viscosity cause a large retardation time, and *vice versa*.

Experimental data sets are fitted to eq. (3) using a nonlinear least-squares technique known as the Levenberg-Marquardt method.⁷ This method is used to find the best-fit parameters τ_k and D_k for a K-V model with multiple elements. Previous work by Weick and Bhushan^{4,5} to determine the viscoelastic characteristics of alternative polymeric substrates used for magnetic tapes showed that two to three elements are typically required for a reasonable fit.

Figure 4 displays how a K-V curve-fit works for one of the experimental data sets, which was acquired at 50°C for a metalized PET sample. A D_0

value of 0.1377 GPa^{-1} is the initial creep compliance for the experiment, and the $\log(0.1377 \text{ GPa}^{-1}) = -0.861$ in the figure. Variation in the data is due to the small temperature cycling in the chamber, which is amplified on the log scale. Application of the Levenberg-Marquardt algorithm results in a six-term, three-element fit as shown in green. If these parameters are separated out and used in pairs as one-element or two-element fits, you get the other trend lines shown in the figure. A relatively small D_1 and τ_1 term fits the initial part of the curve, whereas the larger D_2 and D_3 terms combined with extremely large τ terms fit the latter parts of the data. Note that large positive retardation times cause an increase, whereas negative retardation times cause a decrease. The retardation time can be interpreted as the time required to attain $(1-1/e)$ or 63.2% of the equilibrium strain for each element. For the first element shown in Figure 4, the retardation time is 0.56 h, which corresponds with the curve fit for this line reaching 63.2% of its constant level. One hundred percent of the equilibrium strain occurs at ~ 0.9 h.

Experimental and analytical procedure used for DMA

To help understand the viscoelastic behavior of the tape and substrate materials, an experimental technique known as DMA was used. This technique is sometimes referred to as dynamic mechanical thermal analysis, and subjects small samples of thin polymer films to dynamic stress-strain conditions in a temperature-controlled test apparatus.⁸ When the polymer film samples are subjected to a sinusoidal strain, $\epsilon(t)$, the sinusoidal stress, $\sigma(t)$, measured on the sample reaches peak values at slightly later time periods. This is depicted in Figure 5, and the time lag, Δt , is due to the specific viscoelastic characteristics

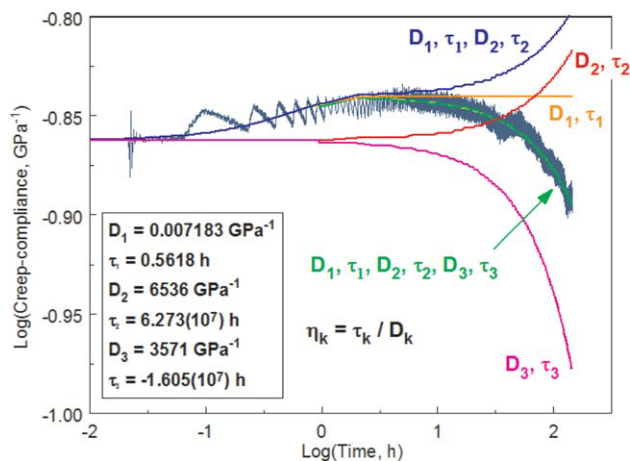


Figure 4 Experimental data for metalized PET (Spaltan[®]) Substrate B sample at 50°C. [Color figure can be viewed in the online issue, which is available at wileyonlinelibrary.com.]

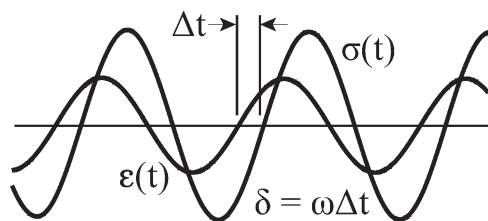


Figure 5 Schematic drawing of sinusoidal strain and stress signals from DMA.

of the polymer film being tested. As shown in eq. (5), a corresponding phase angle shift can be calculated using the frequency of the sinusoidal strain used for the experiment.

$$\delta = (2\pi f)\Delta t \quad (5)$$

where, δ is the phase angle shift, f is the test frequency, and Δt is the time lag between the strain and stress. Using this information, the storage modulus, E' , loss modulus, E'' , complex modulus, E^* , and loss tangent, $\tan(\delta)$ can be calculated using eqs. (6a–d).

$$E' = \cos(\delta) \left[\frac{\sigma}{\varepsilon} \right] \quad (6a)$$

$$E'' = \sin(\delta) \left[\frac{\sigma}{\varepsilon} \right] \quad (6b)$$

$$|E^*| = \sqrt{(E')^2 + (E'')^2} \quad (6c)$$

$$\tan(\delta) = \frac{E''}{E'} \quad (6d)$$

The storage (or elastic) modulus, E' , is a measure of the component of the complex modulus, E^* , which is in-phase with the applied strain, and the loss (or viscous) modulus, E'' , is a measure of the component which is out-of-phase with the applied strain. The in-phase stress and strain results in elastically stored energy that is completely recoverable, whereas out-of-phase stress and strain results in the dissipation of energy that is nonrecoverable and lost to the system. The loss tangent, $\tan(\delta)$, is simply the ratio of the loss (or viscous) modulus to the storage (or elastic) modulus.⁸

A TA Instruments DMA 2980 Dynamic Mechanical Analyzer was used in this study. After the samples were loaded in the grips, the test lengths varied from nominal values of 18 to 20 mm. Multifrequency experiments used to create the 3D graphs presented herein were performed at 0.1, 0.5, 1, 5, and 10 Hz for a -80 to 180°C temperature range with a heating rate of 2°C per min. Samples tested in this manner were first cooled to -80°C , then subjected to the 0.1 to 10 Hz frequency sweep at each temperature interval as the samples were heated-up to 180°C . The separate low-frequency experiments were performed

at 0.05 and 1 Hz frequencies using heating rates of 0.5 and 5°C per min, respectively. The initial oscillation amplitude was set at $16 \mu\text{m}$ with a static force of 0.01 N running in autotension mode set at 125%. The time step between each point was 1.0 s.

RESULTS AND DISCUSSION

Creep-compliance trends

Figure 6 shows the creep-compliance curves generated after fitting the raw data to the K-V model. An average initial creep-compliance, D_o , is used for each curve based on three to four repeat experiments per sample at each of the three temperatures: 30, 50, and 70°C . These D_o values can also be observed in Figure 7 along with the standard deviations. When the average D_o values are subtracted from the creep-compliance data sets, the trend lines take-on more curvature as shown in Figure 8. Note that logarithms of the creep-compliance data in GPa^{-1} are plotted in Figures 6 and 8 as a function of the logarithm of the time in hours to enable the observation of characteristic trends to the curves over extended time periods.

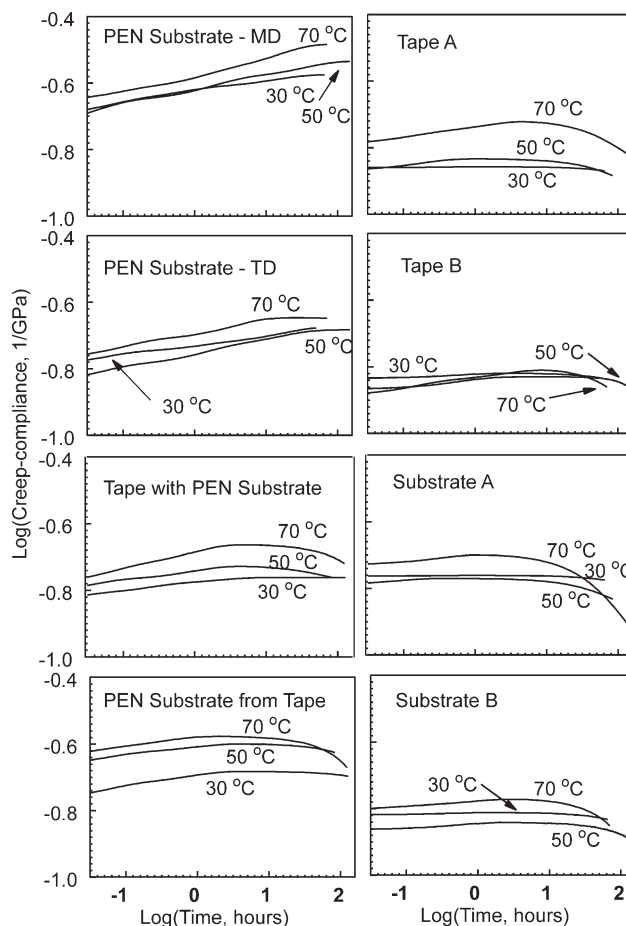


Figure 6 Creep-compliance curve fits for PEN and metalized PET (Spaltan[®]) tape and substrate samples.

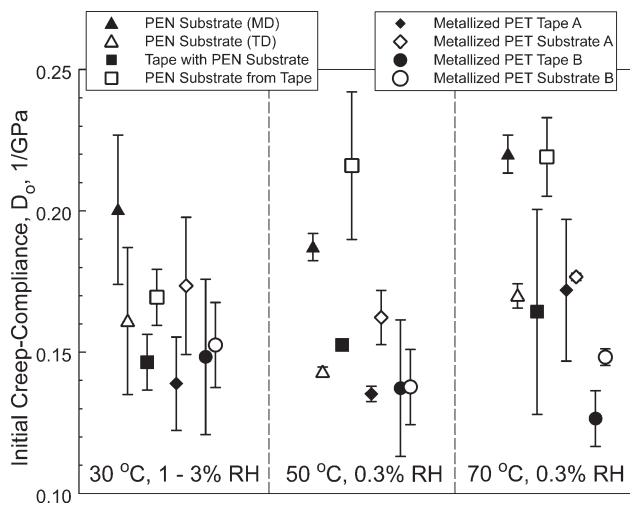


Figure 7 Average initial compliances, D_0 , and standard deviations for PEN and metallized PET (Spaltan[®]) tape and substrate samples.

As shown in Figure 7, PEN-TD has a lower initial creep compliance than PEN-MD at all temperatures, corresponding with TD tensilization and a higher elastic modulus in this direction. The PEN substrate obtained from the tape sample tends to follow the PEN-MD substrate trend, although differences are observed at lower temperatures, and the initial compliance for the PEN substrate also tends to be higher than what was measured for the whole tape. Figure 7 also shows that the metallized PET substrates tend to have similar to higher initial creep-compliance than the corresponding tapes, although standard deviations make this assessment somewhat suspect at certain temperatures. The application of the front coat with a compliant binder system and rigid magnetic particles tends to lower the initial creep compliance, which means the rigid magnetic particles could play a greater role in the initial compliance of these tapes. However, this trend does not continue when the time-dependent creep is considered in Figures 6 and 8. Figure 7 also shows that tapes made from the metallized PET substrates have similar initial creep-compliances with a significant difference only observable at 70°C. The metallized PET tape with the thicker metallized layer (Sample B) tends to have the lowest initial creep-compliance at elevated temperatures, although the metallized PET tape with the thinner metallized layer (Sample A) has a similar initial creep compliance at 50°C. Overlapping error bars at 30°C render the differences between the initial creep compliances for the metallized PET tape samples at this temperature somewhat inconclusive. It should be noted that the 50°C data provides some realistic insight into the creep-behavior of actual tape products stored at this maximum design temperature. The tape with the PEN substrate has a higher initial creep compliance than the metallized

PET tapes at 50°C. Some tape drive manufacturers claim that the initial creep compliance is not an issue, due to the ability of the tape head to servo to different positions. As a result, as shown in Figure 8 it is important to understand the time-dependent creep-compliance response without the D_0 values included.

Compared with other samples in Figure 8, the PEN substrates and tapes tend to have higher overall creep-compliance characteristics when the D_0 values are subtracted out. At longer time periods and higher temperatures, the roll-off occurs that has been observed for other PEN-based substrates and tapes,^{1,3} and it is more prevalent for the PEN substrate obtained from the tape. This is particularly true at the 70°C temperature, although there are minimal differences between the PEN substrate and tape behavior for the 30 and 50°C temperature levels. As was observed for D_0 values plotted in Figure 7, the overall creep-compliance for the PEN-TD sample shown in Figure 8 is still slightly lower compared with the PEN-MD sample when the D_0 values are subtracted out. Additionally, it should be noted

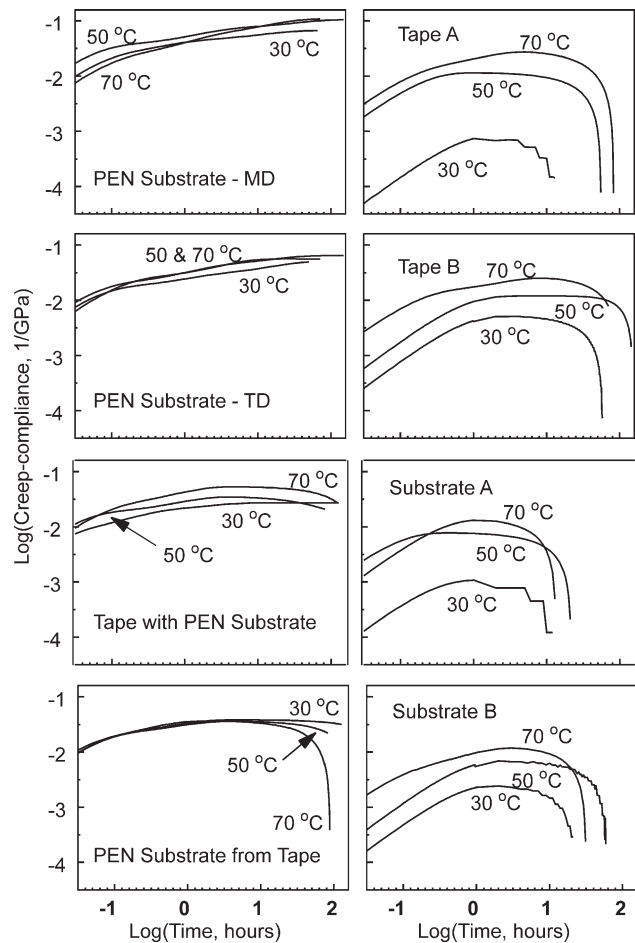


Figure 8 Creep-compliance curve fits for PEN and metallized PET (Spaltan[®]) tape and substrate samples. Average initial compliances, D_0 , subtracted from data sets.

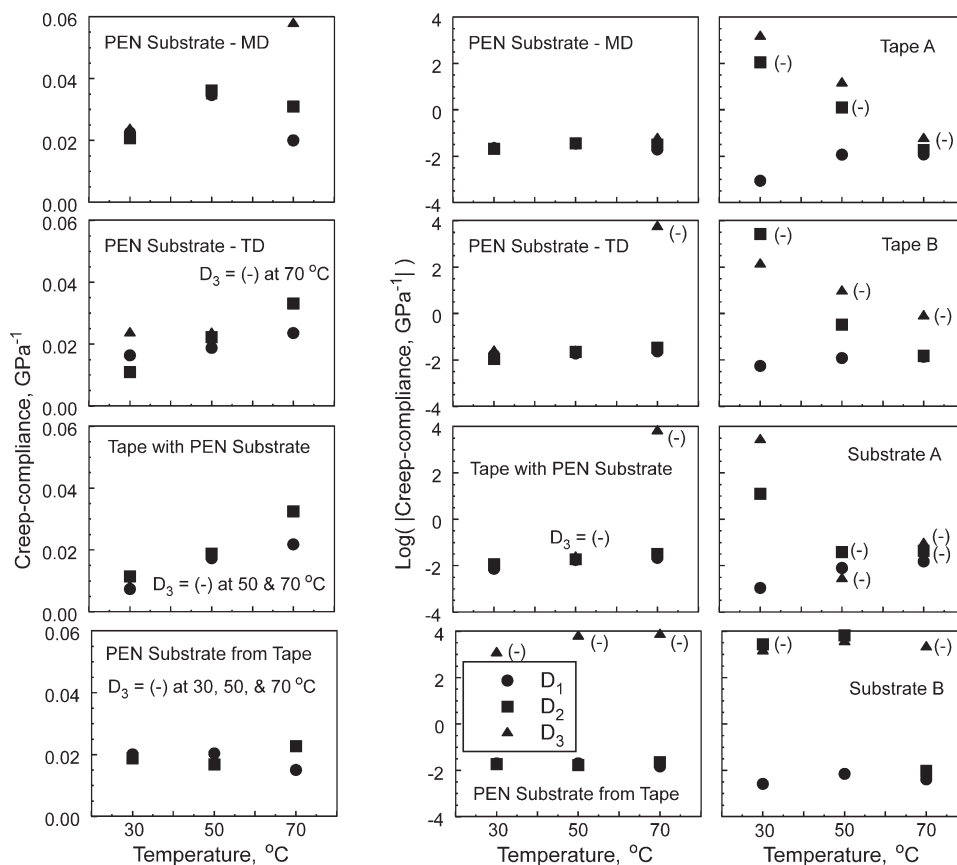


Figure 9 Compliances (D_1 , D_2 , D_3) for PEN samples on linear and log scales compared with those for metalized PET (Spaltan[®]) samples on a log scale.

that at 30 and 50°C the creep-compliance curves for the tape with the PEN substrate are similar to the PEN substrate from the tape, due to a minimal influence of the compliant binder system in the front coat, although as discussed previously, the hard magnetic particles do influence the initial response shown in Figure 7. In comparison, the creep-compliance characteristics of the metalized PET substrates and tapes are significantly different than the characteristics of the PEN substrates and tapes when D_0 is subtracted out. The behavior at different temperatures is also significantly different for the metalized PET substrates and tapes, with higher temperatures leading to higher overall creep compliances in Figure 8. Furthermore, there seems to be a larger increase in creep-compliance when the temperature is increased from 30 to 50°C for Substrate A and Tape A compared with Substrate B and Tape B. This is possibly due to the influence of the thicker metalized layer for Tape B compared with Tape A. Figure 8 also shows only minimal differences between the creep compliance of the substrate versus tape materials. However, the most notable observation from Figure 8 is the characteristic roll-off that is more prevalent in the metalized PET substrates and tapes compared with the PEN substrates and tapes. The roll-off

occurs at all temperatures after ~ 5 to 10 h, although the time that this roll-off begins to occur and drop appears to vary, with significant roll-off occurring after 10 to 50 h. In some cases, the creep-compliance rolls-off to levels lower than what was observed during the initial time periods in Figure 8. Comparisons with DMA data provide insight into this behavior, which could be attributed to relaxations in the predominantly PET substrate.

Curve fit parameters from K-V model

To gain some understanding of the compliance characteristics of the PEN and metalized PET substrates and tapes, individual compliance parameters (D_1 , D_2 , and D_3) are shown in Figure 9. Because of the nature of the data sets for the PEN samples, those plots are shown on both linear and log scales, whereas data sets for the metalized PET samples are only shown on a log scale. The linear scale plots for the PEN-MD, PEN-TD, and PEN tape samples show a generally increasing trend to compliances with the increase in temperature from 30 to 70°C. For each of these samples, the individual compliance parameters (D_1 , D_2 , and D_3) are also similar at 30 and 50°C. For all the PEN samples, at 70°C there is a larger

separation between D_1 , D_2 , and D_3 . This is also true for the PEN tape at 50°C, and PEN substrate from tape at all three temperatures. This corresponds with the roll-off observed in the creep-compliance curves in Figure 8, and can be associated with the D_3 term that tends to go highly positive or negative, which when multiplied by a positive or negative viscosity controls the retardation time. For all samples shown in Figure 9, high-compliance values could drive the influence of the second and third elements to be negligible if one recalls that the retardation time is the product of the intrinsic viscosities and compliances for each element. However, recall from Figure 4 that these relatively high values control the roll-off characteristics. Note that a negative compliance term can be visualized as a retraction of the spring-element rather than an extension. In some contrast to the other PEN samples, the PEN substrate obtained from the tape tends to have negative D_3 values at all temperatures, corresponding to retraction of the sample at longer time periods regardless of temperature, a phenomenon that can be associated with significant shrinkage characteristics of the PEN polymer discussed later in this paper that are possibly enhanced after it is used for tape fabrication.

If only the D_1 values are considered for the metalized PET samples in Figure 9, then Substrate A and B have similar compliance responses at 30°C, but Substrate B with the thicker metalized layer retains a lower compliance response at 50 and 70°C compared with Substrate A. This also tends to be subtly true for Tape B compared with Tape A. Interestingly, the metalized PET substrates and tapes show more of a separation between D_1 , D_2 , and D_3 at 30°C. This could be due to the metalized layers that respond elastically at the low 30°C temperature. However, as the temperature increases, there is a closer correspondence between D_1 , D_2 , and D_3 due to the decreasing influence of the metalized layers. Only Substrate B shows a consistent separation between the parameters, which once again could be attributed to the thicker metalized layer.

When the metalized PET compliances are compared with those determined for PEN, the magnitudes are similar with some exceptions. The metalized PET substrate and tape show more negative compliance responses at 50 as well as 70°C, which corresponds with retraction of the spring element. The magnitude of these compliance extremes corresponds with roll-off of the creep-compliance curves but should be included as a multiplier to the viscosities to determine retardation times in addition to being a multiplier out in front of a K-V term. As was observed in Figures 6 and 8, these characteristics lead to significant differences in creep-compliance behavior for the metalized PET samples compared with the PEN samples. The roll-off tends to be more significant for the metalized

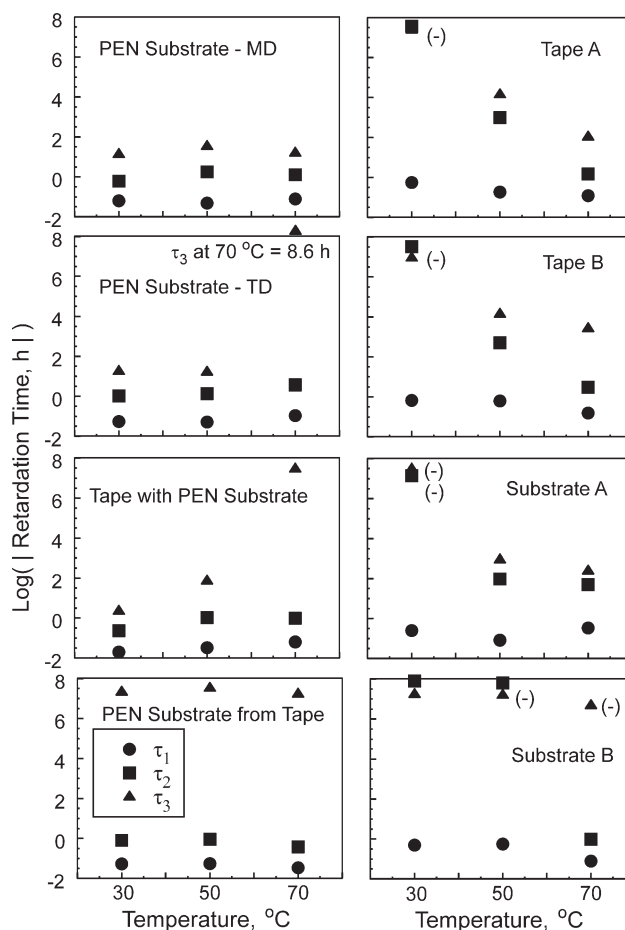


Figure 10 Retardation times (τ_1 , τ_2 , τ_3) for PEN samples compared with retardation times for metalized PET (Spaltan[®]) samples.

PET samples, although the overall compliance response is lower compared with PEN.

A comparison of retardation times can be found in Figure 10. Recall that the retardation time is the time required to attain $(1-1/e)$ or 63.2% of the equilibrium strain for each element. Each k^{th} element of the K-V model contributes a delayed compliance of magnitude $D_k[1-\exp(-t/\tau_k)]$, and the amount of this delay is directly related to the magnitude of the retardation times τ_k . Retardation times for the PEN substrates and tape tend to build with each consecutive element, and reach peaks at 50 or 70°C. In general, extreme retardation times correspond with downward roll-off of the curves, and extreme τ_1 and τ_2 values for the metalized PET samples at 30°C correspond with the elastic behavior observed for these samples at lower temperatures. Substrate B and Tape B seem to retain this characteristic more at higher temperatures compared with the Substrate A and Tape A samples due to the thicker metalized layer used for the B samples. When compared with the PEN samples, the metalized PET samples appear to have higher τ_1 values at 30 and 50°C. This is less prevalent at 70°C, but roll-off characteristics for both

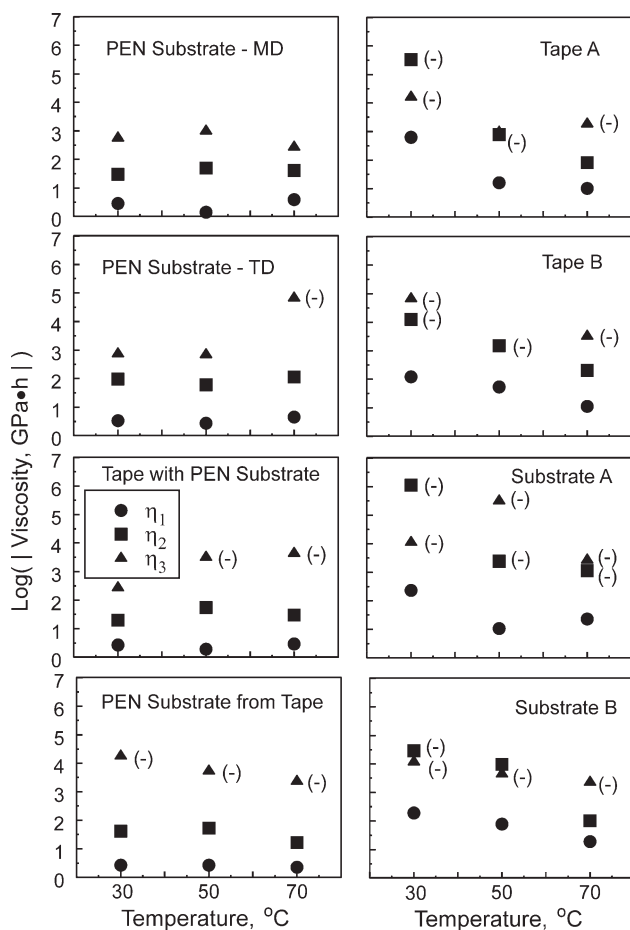


Figure 11 Viscosities (η_1 , η_2 , η_3) for PEN samples compared with viscosities for metalized PET (Spaltan[®]) samples.

types of substrates are more dominant at this temperature due to the influence of both the retardation and compliance values for the second and third K-V elements noting that the retardation time is really a derived quantity that is equal to the compliance times the viscosity for each element.

As was observed for the retardation times in Figure 10, the viscosities for the PEN substrates and tape in Figure 11 tend to build with each consecutive element, and reach peaks at 50 or 70°C. Extreme viscosities also correspond with roll-off of the curves. In cases where a compliance term is negative and the retardation time is positive, the viscosity is negative, which means the piston is moving in the opposite direction in the dashpot when the mechanical K-V analogy is utilized. There are more negative viscosities at all temperatures for metalized PET compared with the PEN samples. This accounts for attenuation of the overall creep behavior at lower temperatures and roll-off at higher temperatures for these samples. When the η_1 values are considered alone for the metalized PET samples, they tend to be higher than what was measured for PEN samples. This supports the notion of an increase in viscous (or decrease in fluid-like behavior) for metalized PET substrates and tapes compared with

PEN substrates and tapes due to the presence of the more rigid metal layer.

The η_1 values for Substrate B are similar to η_1 values for Substrate A, which suggests the thickness of the metal coating does not have a large influence on attenuating the fluid-like behavior of the underlying PET substrate during shorter time periods. However, contrary to this observation is the presence of the more negative η_2 and η_3 values for Substrate A compared with Substrate B, which suggests that the thicker metalized coating helps to prevent the more prevalent roll-off characteristics observed for Substrate A compared with Substrate B. This uses the notion stated earlier for highly negative retardation times and associated negative viscosities, which cause substantial roll-off at higher temperatures and/or longer time periods. Lastly, it is interesting to note that the viscosity characteristics for Tape A and Tape B are pretty similar, which suggests that the front and back coats of the tape play an important roll in moderating the creep behavior of the metalized PET substrates.

DMA of substrates

General observations—temperature and frequency dependence

Figure 12 shows DMA results for the PEN substrates cut from wide stock in the MD and TD direction as well as the PEN substrate obtained from a tape sample after removing the front and back coats of the tape. Figure 13 shows DMA results for the two metalized PET substrates that were also obtained from tape samples by removing front and back coats of the tape. The storage modulus (E'), loss modulus (E''), and $\tan(\delta)$ are plotted from top to bottom in each column as a function of temperature in °C and the log of frequency in Hz. Color bars shown at the right of each figure can be used to determine magnitudes in addition to the vertical tick marks. For each substrate type, only one sample was used for each experiment using the settings noted in the Introduction. The sample was first cooled down to 80°C before being pulled at each frequency interval of 0.1, 0.5, 1, 5, and 10 Hz. Then, it was heated to the next temperature level at a rate of 2°C/min, and the multiple frequency measurements were repeated. This process continued until the final 180°C temperature level.

As expected for the storage modulus (E') plots, there is a decreasing trend to the storage modulus as temperature increases from -80 to 180°C. From Figure 12, PEN substrates cut in the MD and TD directions from wide-stock have similar storage modulus characteristics, which is likely due to biaxial tensilization used to make the samples. In comparison, the PEN substrate obtained from the tape

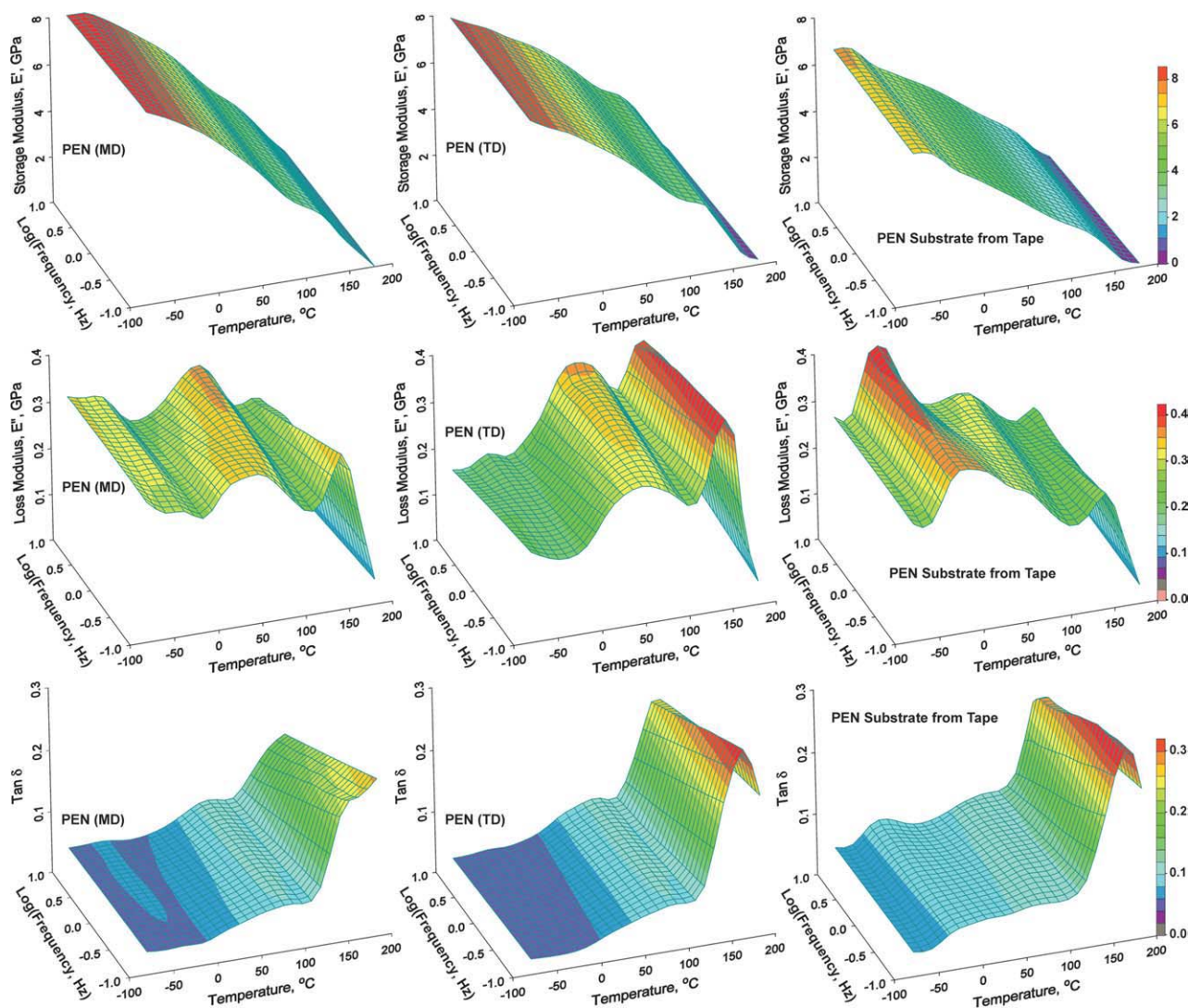


Figure 12 DMA results for PEN substrate samples cut from wide-stock in the MD and TD along with results for a PEN substrate sample from a magnetic tape. Storage moduli, loss moduli, and $\tan(\delta)$ results are shown for each sample as a function of frequency and temperature. [Color figure can be viewed in the online issue, which is available at [wileyonlinelibrary.com](http://www.interscience.wiley.com).]

sample has a slightly lower overall storage modulus as a function of temperature. Storage modulus plots in Figure 13 for the metalized PET substrates also show a slightly lower overall storage modulus, but the curves tend to flatten-out in the middle temperature range before decreasing. Note that none of the storage modulus plots for the PEN or metalized PET substrates show a significant change with frequency for the 0.1 to 10 Hz frequency range used in the study. However, there is a slight increase in storage modulus observed with an increase in frequency for all samples.

The second row of panels in Figures 12 and 13 show the Loss Modulus (E'') plots as a function of frequency and temperature for the substrates evaluated in this study. These plots are reoriented in Figure 14 as two dimensional plots with E'' as the vertical axis and temperature in $^{\circ}\text{C}$ as the horizontal

axis. Peaks are also labeled in Figure 14 as β , β^* , and α . Only the PEN substrates have the β^* peaks, whereas both the PEN and metalized PET samples have both the β and the α peaks. The β peaks correspond with short-range motions of the ester groups in the polyester backbones of PEN and PET, whereas the α peaks correspond with long-range motion in the amorphous region often referred to as the glass transition.⁹ As discussed by Tonelli,¹⁰ the β^* peak that is unique to PEN is due to rotation of the naphthalene ring, and Weick¹ provides a discussion of this phenomenon as it relates to PEN-based magnetic tapes. It is interesting to note that the β^* peaks are most prevalent in the PEN MD and TD samples, but the PEN substrate from the tape sample has a very prevalent β peak compared to both the β^* and α peaks. This could be a peculiarity due to the processing of the tape, and a comparison with shrinkage

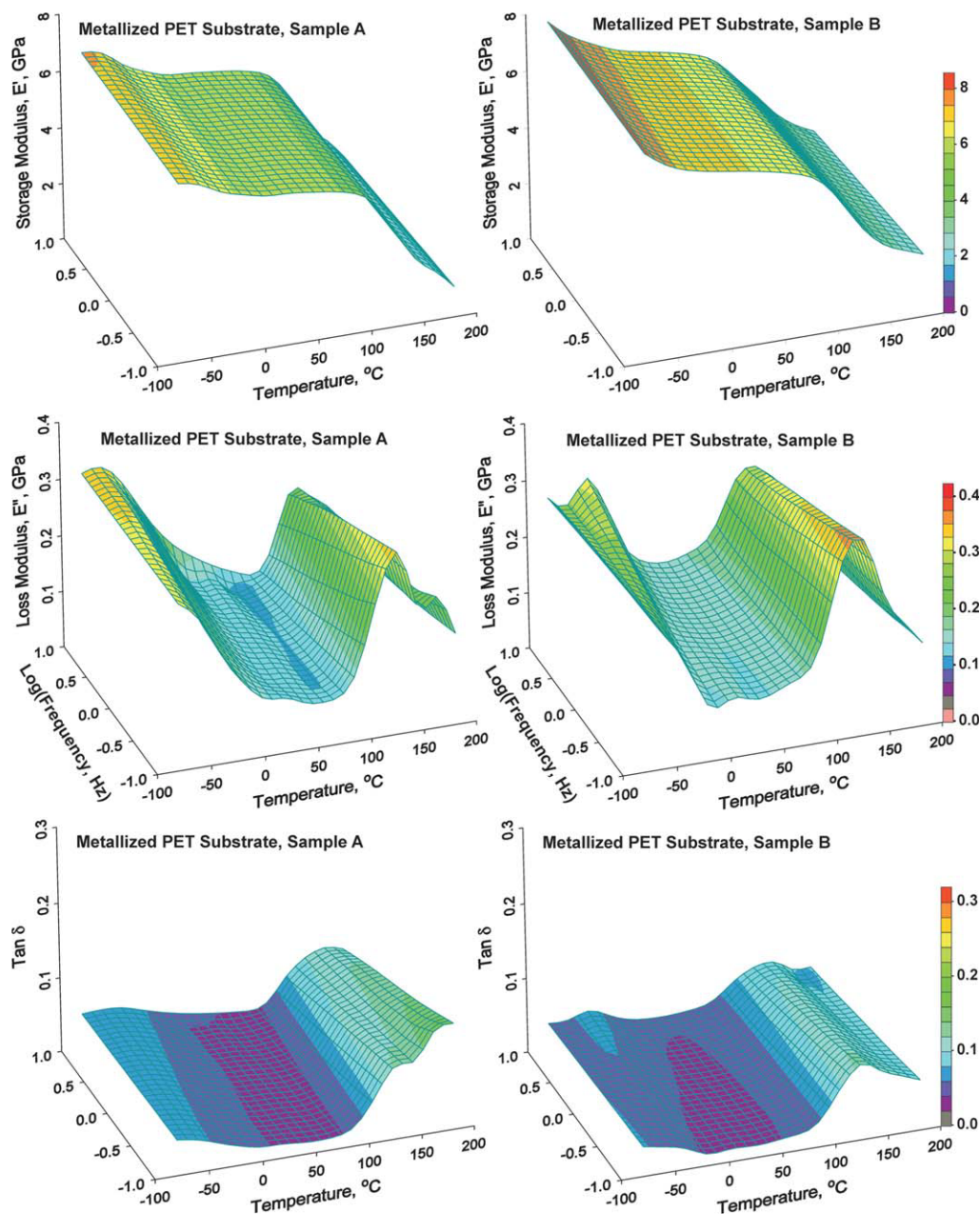


Figure 13 DMA results for metallized PET (Spaltan[®]) substrate samples from magnetic tapes. Storage moduli, loss moduli, and $\tan(\delta)$ results are shown for each sample as a function of frequency and temperature. [Color figure can be viewed in the online issue, which is available at wileyonlinelibrary.com.]

and creep data are discussed later in this article. Such comparisons can also shed light on why the β peaks in the metallized PET samples are also very prevalent.

By calculating the ratio of the loss modulus to the storage modulus, the $\tan(\delta)$ plots can be generated. Due to the large magnitude of the storage modulus relative to the loss modulus, the peaks tend to be attenuated. As a result, the β and β^* peaks disappear, whereas the large α peaks are more prevalent. Although the α peaks are also present in the loss modulus plots, their higher magnitude relative to other peaks in the $\tan(\delta)$ plots has led scientists to

use their location in the $\tan(\delta)$ plots as a measurement of the glass transition temperature. Therefore, based on these $\tan(\delta)$ plots, the PEN substrate obtained from the tape sample has a higher glass transition temperature of $\sim 160^\circ\text{C}$ compared to $\sim 125^\circ\text{C}$ measured for the metallized PET B substrate. However, the frequency dependence of these peaks and whether they are narrow or broad needs to be considered.

Peak locations and shifts with frequency

For archival purposes, magnetic tapes are stored in a $16\text{--}32^\circ\text{C}$, $20\text{--}80\%$ RH environment,² and it is important

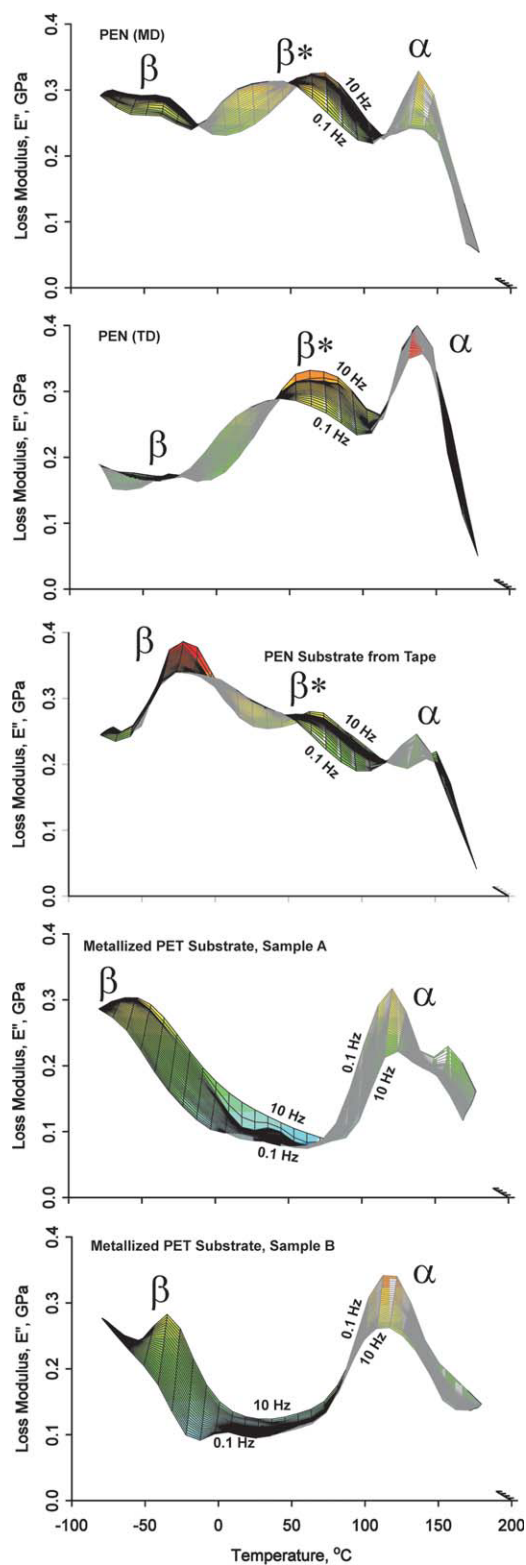


Figure 14 Loss modulus versus temperature results from DMA of PEN substrates samples cut from wide stock in the MD and TD directions along with results for a PEN substrate sample from a magnetic tape and metallized PET (Spaltan[®]) substrate samples from magnetic tapes. [Color figure can be viewed in the online issue, which is available at wileyonlinelibrary.com.]

to understand properties and characteristics for this temperature and humidity range. Because DMA is performed at relatively high frequencies, and dimensional instabilities associated with viscoelastic creep mechanisms occur at comparatively low frequencies, it is useful to understand how the transition phenomena measured by the peaks in DMA measurements shift with frequency. Figures 12 and 13 show some evidence of the effects of frequency, but the E'' versus temperature plots in Figure 14 provides a better understanding of how the peaks shift with a change in frequency. Recall that these experiments were performed using a single sample, and frequency sweeps from 0.1 to 10 Hz were performed at each temperature level as the sample was warmed from -80 to 180°C . To further understand how the transition peaks shift with frequency, additional experiments were performed using the same -80 to 180°C range, but one sample was pulled at 0.05 Hz, and a second sample was pulled at 1 Hz. A finer temperature resolution of 0.25 and 0.50°C could be used at these specific test frequencies, and E' , E'' , and $\tan(\delta)$ results are shown in Figures 15 and 16 for the substrate samples used in this study.

Based on the E'' data shown in Figure 14, the α peak location for the PEN-based samples seems to show no shift with temperature for the 0.1 to 10 Hz range, with only a minimal decrease in magnitude in Figure 12. Based on the E'' data, the location of the α peak is at 137°C for the PEN-based samples. In comparison, from Figure 14 the α peak location for the PET-based samples does shift slightly to a higher temperature at 10 Hz from its peak at 120°C at 0.1 Hz. The magnitude of this peak also decreases slightly with an increase in frequency. The presence of the β^* peak is unique to the PEN-based samples due to the naphthalene ring, and it shifts to lower temperatures with a decrease in frequency. For all three PEN substrate samples, at 10 Hz the β^* peak is located at 71°C , and shifts to 48°C at 0.1 Hz, although this peak at the lower frequency is only predominant for the PEN (MD) and (TD) samples, and seems to be blended into the β peak for the PEN substrate sample that was obtained from the tape. For all the samples, the β peaks at subzero temperatures show minimal shift in the 0.1 to 10 Hz frequency range, although their magnitudes do tend to decrease with a decrease in frequency.

Storage modulus (E') data shown in Figures 15 and 16 for the 0.05 and 1 Hz test frequencies typically show a decrease in magnitude with a decrease in frequency. Only the PEN (MD) data sets show the opposite trend. It is also interesting to note the E' values at 25°C are 4.2 and 3.4 GPa for PEN (MD) tested at 0.05 and 1 Hz, whereas the E' values at 25°C for PEN (TD) are 3.7 and 6.4 GPa. The E' values at 25°C for the PEN substrate from the tape are

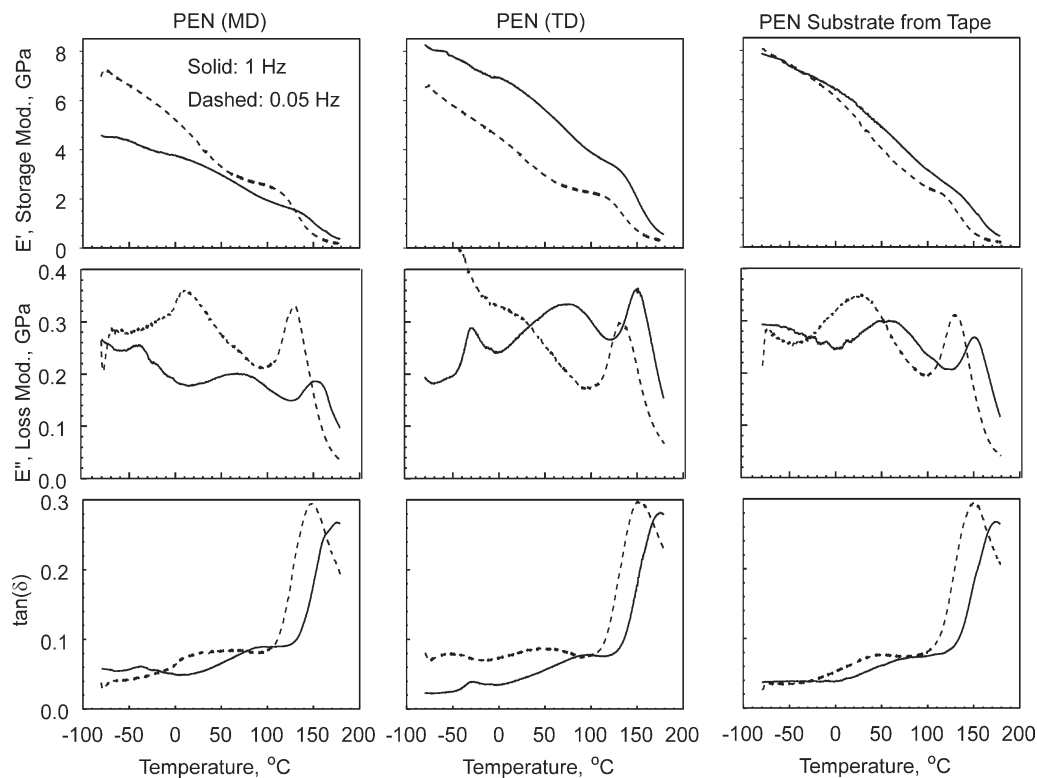


Figure 15 Comparison of DMA results at two frequencies (0.05 Hz and 1 Hz) for PEN substrate samples cut from wide stock in the MD and TD along with results for a PEN substrate sample from a magnetic tape.

5.1 and 5.7 GPa at 0.05 and 1 Hz. In comparison, the E' values for metallized PET Substrate A at 25°C are 4.5 and 5.4 GPa at 0.05 and 1 Hz, and 3.2 and 4.3

GPa for metallized PET Substrate B at 0.05 and 1 Hz. Furthermore, it is interesting to note the flatter E' curves for the metallized PET samples, particularly in the intermediate temperature range.

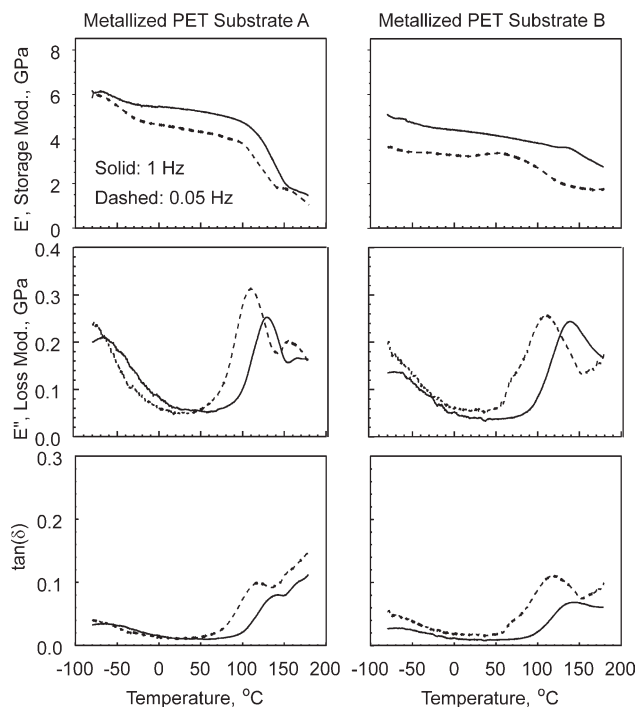


Figure 16 Comparison of DMA results at two frequencies (0.05 Hz and 1 Hz) for metallized PET (Spaltan®) substrate samples from magnetic tapes.

Peak shifts with frequency are much more prevalent for the loss modulus (E'') data shown in Figures 15 and 16. The α peak shifts from 150°C at 1 Hz to 130°C at 0.05 Hz for the PEN based samples, and from 130°C at 1 Hz to 110°C at 0.05 Hz for metallized PET Substrate A, or 140°C at 1 Hz to 110°C at 0.05 Hz for metallized PET Substrate B. In short, a $\sim 20^\circ\text{C}$ downward shift in the location of the α peak occurs for PEN and PET-based substrates, with the α peak locations always at higher temperatures for the PEN substrates. Note that the α peak locations measured with the $\tan(\delta)$ plots are somewhat higher, and occur at 172 and 150°C for the 1 and 0.05 Hz test frequencies used for the PEN substrate samples. In comparison, these peaks are at 140 and 120°C for the PET-based substrates. Note that α peak locations from the $\tan(\delta)$ plots are commonly used for glass transition temperature specifications, and it is interesting to note that these “specifications” are not constant with frequency.

The location of the β^* peaks for the PEN substrates in Figure 15 is lower for 0.05 Hz compared with the 1 Hz test frequency, which is similar to the trends observed in Figures 12 and 14 for the 0.1 to 10 Hz test frequencies. For the PEN (MD) and (TD)

substrates, the shift is from 75 to $\sim 10^\circ\text{C}$ for the 1 and 0.05 Hz test frequencies, although the location of the β^* peak at 0.05 Hz for the PEN (TD) sample is unclear since it appears to merge with the location of the β peak. Interestingly the specific locations of the β^* peak for the PEN substrate obtained from the tape appears to be at 60 and 25°C for the 1 and 0.05 Hz test frequencies, which is a narrower range and at slightly different locations compared with the PEN wide stock samples. Note that the magnitude of the β^* peaks also increases with a decrease in test frequency.

Although somewhat observable in the E'' and $\tan(\delta)$ curves at 1 Hz for both the PEN and PET substrate samples, the β peaks at subzero temperatures appear to be typically off-scale at the lower 0.05 Hz test frequencies. Some slight increases at -80°C should not be misinterpreted as peaks, and could be due to anomalies that occur during the start of the experiment. Overall magnitudes of the β peaks are also somewhat inconsistent, with off-scale magnitudes for the PEN (TD) samples. However, similar peak magnitudes were measured for the other PEN substrate samples with slight lower β peak magnitudes for the PET substrate samples, but once again actual peak locations seem to be off-scale for some PET samples.

Shrinkage

In addition to the creep behavior at elevated temperatures due to dimensional changes from the application of an external stress, polymer materials such as the polyester substrates used in this study undergo another type of dimensional change at elevated temperatures call shrinkage. This behavior is independent of the applied stress, and causes the polyester substrate to contract if a strip of it is held between two fastening points at an elevated temperature. This type of phenomena has been measured for both PET and PEN substrates,⁶ and has been attributed to movement of partially oriented molecules in the amorphous regions at elevated temperatures. This movement leads to a contraction of the partially-oriented molecules in the amorphous phase, and contraction or shrinkage of the ultra-thin tape or substrate material.

To measure shrinkage with the custom creep apparatus, a minimal 0.5 MPa stress is used to keep the samples tight between the grips. Then, the test chamber is brought up to test temperature, and the change in length of the samples is measured in the same manner it is measured during the creep experiments. However, instead of undergoing a positive change in length associated with creep, the samples contract or shrink over an extended time period at the elevated test temperature.

Figure 17 provides shrinkage results for the wide-stock PEN samples cut in the MD and TD as well as

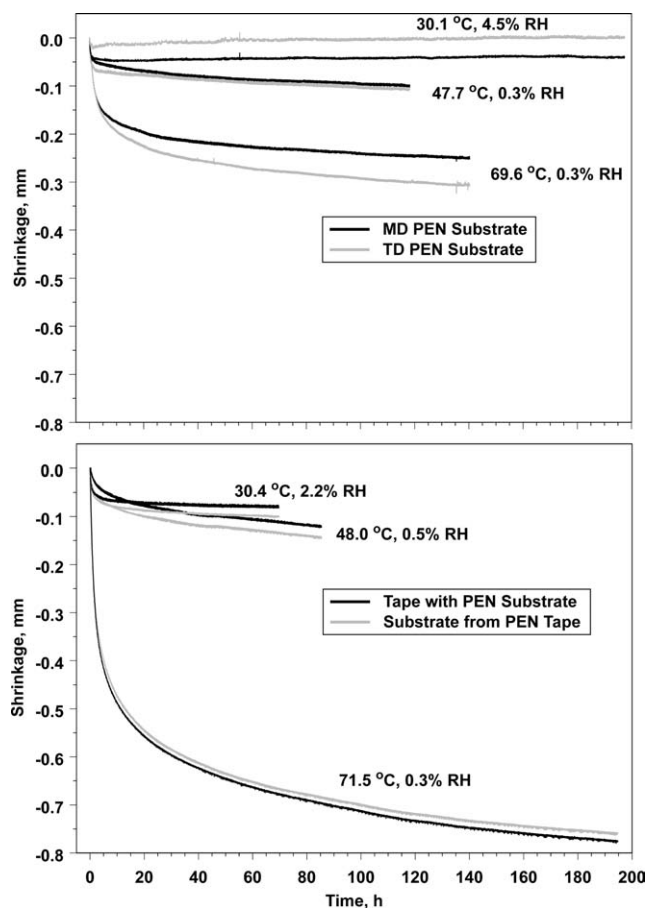


Figure 17 Shrinkage results for PEN substrate samples cut from wide stock in the MD and TD along with results for a PEN substrate sample from a magnetic tape.

results for the PEN based tape and substrate. The PEN tape and substrate acquired by removing the front and back coats from the tape show the largest amount of shrinkage at 70°C , which is why the experiments were continued out to almost 200 h to show that this behavior would continue over an extended time period. Although the PEN tape showed a slightly larger amount of shrinkage than the substrate, the samples shrank a similar amount, which means the behavior is dominated by the substrate and the contribution from the front and back coat is minimal. In comparison, shrinkage of the PEN MD and TD wide stock samples is lower at 70°C with the TD sample showing slightly larger shrinkage than the MD sample. Results at 50°C are similar for the PEN samples, although the PEN tape and substrate tend to show a slightly steeper slope than the PEN MD or TD samples. At 30°C shrinkage is minimal compared with the higher temperatures, and there tends to be a leveling-off of the shrinkage results after the initial few hours of the experiments. Overall, the PEN MD and TD samples show less shrinkage at 30°C than the PEN tape or substrate

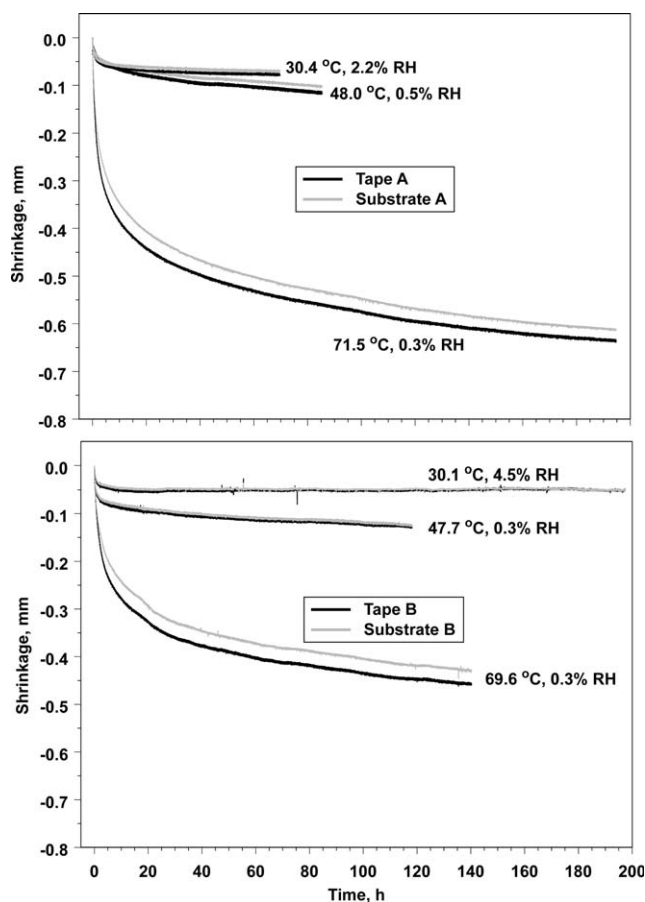


Figure 18 Shrinkage results for metalized PET (Spaltan[®]) tape and substrate samples.

sample, with the shrinkage of the PEN TD sample being almost immeasurable.

Shrinkage results for the metalized PET tapes and substrates are shown in Figure 18 for the 30, 50, and 70°C test temperatures. As observed for the PEN tape versus substrate samples, the tape samples tend to shrink more than the substrate samples, although the difference is small. This means that the shrinkage behavior is dominated by the substrate behavior. However, the presence of the thicker metalized layer for the B samples tends to lead to a lower amount of shrinkage compared with the A samples that have the thinner metalized layer. The experiments at 70°C clearly show the difference between the A and B metalized PET samples, whereas there is less of a difference at 50 and 30°C, although the shrinkage of the B samples still tends to be lower than the A samples at these temperatures.

Comparisons of shrinkage behavior between the two types of polyester samples can also be made using the results shown in Figures 17 and 18. The PEN tape and substrate sample acquired by removing the front and back coats of the tape show the largest amount of shrinkage compared to any of the other samples. However, the metalized PET samples show a larger amount of shrinkage than the PEN

MD and TD samples cut from wide stock. Note that these observations are particularly true at 70°C, but also tend to occur at the lower 50 and 30°C test temperatures. One could argue that the naphthalene ring structure in the PEN samples makes it more difficult for this material to crystallize, and therefore more partially oriented PEN molecules are left in the amorphous region leading to a larger amount of shrinkage. However, this statement would only explain the larger shrinkage for the PEN tape and substrate materials compared with the metalized PET materials. Since the PEN MD and TD samples do not shrink as much as the samples that are either tapes or substrates obtained from the tapes, then processing of the tape is likely to lead to some unintentional postprocessing of the underlying substrate material. Although specific processes and temperatures are proprietary, it is reasonable to assume that the elevated temperatures needed to coat the substrate with the front coat (magnetic + nonmagnetic layers) in addition to the back coat perhaps leads to some partial disorientation of molecules from the crystalline region to the amorphous region. As a result, these partially oriented molecules contract leading to shrinkage of the tape and substrate materials during the experiments shown in Figures 17 and 18. If the PEN MD substrates from wide stock were used to make tapes, then it is reasonable to assume that the shrinkage of the resulting tape would be greater and similar to the PEN tape and substrate results in Figure 17.

CONCLUSIONS

Metalized PET (Spaltan[®]) tapes and substrates do tend to have lower initial creep compliances, D_0 , than PEN tapes and substrates, but this should not be used as the sole criteria for specifying a substrate just as the elastic modulus or even T_g should not be used in this manner. Instead, a more thorough approach should be taken that accounts for the time and temperature-dependent viscoelastic behavior that lead to dimensional stability problems. Parameters determined from fitting creep data to generalized K-V models provide insight into the dimensional stability behavior and composition of the substrate and tape materials. Correlations with DMA data trends could provide even more insight, and shrinkage characteristics also need to be accounted for.

Negative compliance parameters correspond with retraction and shrinkage of the samples. This can not only attenuate creep, but can also lead to roll-off of the creep-compliance curves at extreme negative magnitudes. Each compliance parameter is a multiplier to a respective viscosity parameter that determines a retardation time for a K-V element, and each compliance parameter is also a multiplier out

in front of each K-V element. The D_3 terms for PEN substrates and tapes can be highly negative at 50°C and particularly 70°C. The PEN substrate tested even showed this D_3 response at 30°C. η_3 viscosity terms for PEN determined by $\eta_3 = \tau_3/D_3$ also follow this negative trend. This corresponds with roll-off of the creep response. β^* peaks indicate rotation of the naphthlene rings and associated functional groups, which occurs in this temperature range, particularly at lower frequencies, and even the α peak shift to lower temperatures at lower frequencies could be correlated with the creep-compliance roll-off.

More compliance and viscosity terms tend to be negative for metalized PET (Spaltan[®]) compared to PEN, with Substrate sample B showing more negative compliance parameters, and Substrate sample A showing more negative viscosity parameters. Interestingly, tapes made with Substrates A and B have similar compliance and viscosity characteristics. As observed for the PEN sample, DMA results show that the α peak shift to lower temperatures at lower frequencies could be correlated with the roll-off observed for these samples.

Shrinkage characteristics for the metalized PET and PEN tapes and substrates seem to be more prevalent after the coating operations when the front coat (magnetic and nonmagnetic layers) plus back coat are applied. The lowest amount of shrinkage was measured for the MD and TD samples cut from wide stock PEN, which had not yet been used for processing. It is interesting to note that large β peaks measured at subzero temperatures from DMA seem to correspond with large amounts of shrinkage. Despite the fact that the shrinkage and DMA results are performed at different temperatures, it is important to note that the β peaks in the DMA results correspond with motion of the ester linkages in the molecular chains. And, interaction between ester linkages in opposing chains contributes to intermolecular bonds between the chains, which are broken and reformed during shrinkage as the partially oriented molecules contract in the amorphous region. Furthermore, large amounts of roll-off in the creep-compliance curves after long time periods at elevated temperatures corresponds with more pronounced shrinkage behavior. The metalized PET and PEN tape samples exhibited this behavior as did the substrates extracted from these tapes. Therefore, shrinkage phenomena associated with contraction of the extended polyester chains could be contributing to the roll-off behavior observed in the creep-compliance measurements at extended time periods for these samples and the negative viscosity and compliance parameters that are typically associated with this roll-off behavior. Energy dissipated through viscous mechanisms in the amorphous regions of the polyester substrates seems to lead to the dimensional instabilities,

and partially oriented molecules in these amorphous regions seem to contribute to these instabilities.

Processing methods appear to influence the dimensional stability of finished magnetic tape. The uncoated substrates themselves exhibit creep and shrinkage behavior that is tightly controlled by the practices of the tape substrate manufacturer. However, dimensional stability of the finished tape is also highly influenced by processing conditions used to coat the substrate with the front coat (magnetic plus nonmagnetic layers) as well as the back coat. This coating process is performed at high speeds on sheets typically 400–800 mm wide moving through rollers, tension control bars, coaters, driers, and inline calendar rolls, which subjects the newly formed tape to a complex stress state. The tape is then wound onto large bulk rolls and cured for up to 20 h at elevated temperatures (typically 40–50°C) under relatively high pack pressures if large diameter hubs are used. Some manufacturers use rigid metal hubs whereas others use compressible paper hubs. In addition, some manufacturers wind these bulk rolls with the coating side up, whereas others wind the rolls with the coating side down. Variables such as these can lead to the dimensional stability issues observed for magnetic tapes such as those evaluated in this study. With relaxations such as the β^* and α transitions occurring at or near room temperature depending on the rate or time period of deformation, it is important for media manufacturers to determine methods to minimize and control mechanical properties of the as-produced tape to enable the successful use of future more advanced tapes with higher densities for long-term archival storage applications.

The author thanks the members of the INSIC Tape Program for their support and valuable input throughout the course of the research activity; W. Imano and T. Magbitang at the IBM Almaden Research Center for providing access to their Dynamic Mechanical Analysis equipment; and Sony and Teijin-Dupont for providing samples for this research.

References

1. Weick, B. L. *J Appl Polym Sci* 2009, 111, 899.
2. IBM/TO Ultrium 4 800 GB Data Cartridge; IBM Systems and Technology Group: Somers, New York, 2007.
3. Weick, B. L. *J Appl Polym Sci* 2006, 102, 1106.
4. Weick, B. L.; Bhushan, B. *J Inf Stor Proc Syst* 2000, 2, 1.
5. Weick, B. L.; Bhushan, B. *J Appl Polym Sci* 2001, 81, 1142.
6. Weick, B. L.; Bhushan, B. *J Appl Polym Sci* 1995, 58, 2381.
7. Press, W. H.; Flannery, B. P.; Teukolsky, S. A.; Vetterling, W. T. *Numerical Recipes in C: The Art of Scientific Computing*; Cambridge University Press: New York, 1988.
8. Aklonis, J. J.; MacKnight, W. J. *Introduction to Polymer Viscoelasticity*; Wiley: New York, 1983.
9. Canadas, J. C.; Diego, J. A.; Mudarra, M.; Belana, J.; Diaz-Calleja, R.; Sanchis, M. *J Polymer* 1999, 40, 1181.
10. Tonelli, A. E. *Polymer* 2002, 43, 637.